Impact of the angle of attack of longitudinal vortex generator on enhancement heat transfer for a wavy-fin compact heat exchanger with circular and elliptical tubes

Laís S. Bandini[1], Leandro O. Salviano[2]

[1]*Dept. of Mechanical Engineering, Thermal Science Area, São Paulo State University*
Brasil Sul Avenue - 56, 15385-000, Ilha Solteira/ São Paulo, Brasil
lais.bandini@unesp.br
[2]*Dept. of Mechanical Engineering, Thermal Science Area, São Paulo State University*
Brasil Sul Avenue - 56, 15385-000, Ilha Solteira/ São Paulo, Brasil
leandro.salviano@unesp.br

Abstract. The growing industrial development over the last decades led to the improvement of several thermal devices. Among the main types of equipment that have evolved in the last decades, heat exchangers stand out. The present work investigates the heat transfer augmentation for a wavy-fin compact heat exchanger operating at low Reynolds numbers, by combining longitudinal vortex generators. The computational modeling considers a tridimensional model, for an incompressible, steady-state and turbulent flow. The heat exchanger with wavy fins is evaluated considering circular and elliptical tubes for staggered arrangement combined with vortex generator of delta-winglet and rectangular-winglet with aspect ratio of 2 and angles of attack of 15º, 30º and 45º. The heat transfer was evaluated by Colburn Factor and the pressure drop by Friction Factor. In comparison with the reference heat exchanger (without vortices generators), the results show an increase in the heat exchange of 41% using the elliptical tubes associated with a rectangular-winglet vortex generator at the angle of attack of 45º. For the friction factor, the configuration with rectangular-winglet vortex generators is higher than delta-winglet vortex generator independently of the angle of attack. Moreover, the friction factor for circular tubes is higher than elliptical tubes. Overall, the results showed that the compound passive technique is an efficient technique to improve the heat exchange in the compact heat exchanger, allowing, among others things, the reduction of materials for fabrication process and manufacturing.

Keywords: Longitudinal Vortex Generator, Compact Heat Exchanger, Computational Fluid Dynamics, Wavy-fin.

1 Introduction

Heat exchangers are used to providing heat transfer between two or more fluids with different temperature. These devices are widely used in many industries and applications, including the process and chemical industries, transportation, air conditioning and refrigeration [1]. High-efficiency heat exchangers can reduce the cost of materials, energy consumption and also to mitigate the environmental impacts [2].

For the past decades, several techniques have been developed to improve the thermal efficiency of heat exchangers [3]. These techniques are named Active and Passive techniques. Active techniques involve the use of external power to augment the heat transfer rate, while passive techniques do not require any external power to enhance the heat transfer performance of heat exchangers [4].

To improve performance and meet the demands for high efficiency and low cost devices, the most common way to reach it is to use passive techniques, such as heat transfer surfaces able to periodically interrupted the dynamic and thermal boundaries layers along the flow direction [5]. Wavy-fin and longitudinal vortex generators are typical and efficient example of surface applied to enhance the heat transfer of compact heat exchanger [6].

These mechanisms for increasing heat transfer are generally to disrupting the growth of the boundary layer, to increase turbulence intensity and to generate secondary flow such as eddies or vortices [7]. Normally, the increase in heat transfer rate is accompanied by an increase in pressure drop, increasing by pumping power [8]. In Fig. 1 it is possible to observe the waved geometry of the compact heat exchanger.

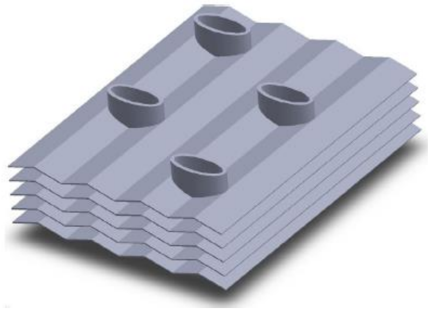

Figure 1. Geometry of the wavy fin of the heat exchanger. [9]

In the present research, a modeling and numerical simulation of a wavy-fin compact heat transfer with a longitudinal vortex generator is performed, using Computational Fluid Dynamics (CFD), considering a wavy-fin compact heat exchanger with circular and elliptical tubes combined with vortex generator. Vortex generator type delta-winglet and rectangular-winglet with aspect ratio of 2 and angles of attack of 15º, 30º and 45º are investigated for staggered arrangement tubes. The operational range is similar to found in refrigeration applications and air conditioning, corresponding to Reynolds number from 150 to 600 (based on Fin Pitch).

2 Governing equations and thermal-hydraulic parameters

The flow is considered turbulent, steady-state, three-dimensional and incompressible flow with constant properties, according to Bhutta et al. [10]. Being an air flow with Prandt number 0,7. The governing equation of conservation of mass, momentum and energy are shown below.

$$\frac{\partial}{\partial x_j}(\rho u_j) = 0. \tag{1}$$

$$\frac{\partial}{\partial x_j}\left(\rho u_j u_i - \tau_{ij}\right) = -\frac{\partial p}{\partial x_i}. \tag{2}$$

$$\frac{\partial}{\partial x_j}\left(\rho u_j h - k\frac{\partial T}{\partial x_j}\right) = -u_j\frac{\partial p}{\partial x_j} + \tau_{ij}\frac{\partial u_i}{\partial x_j}. \tag{3}$$

where: u is the velocity component, h is the convection heat transfer coefficient, x_{i} and x_{i} are generalized coordinates, p is pressure, τ_{ii} is tension tensor, ρ is density, k is thermal conductivity and T is temperature.

The Ansys Fluent 19.0 was used to solve the governing equations, which is a finite volume-based commercial software [11]. The flow is considered turbulent, even though a low Reynold number value is verified, due to instability effects and secondary flow, both introduced by the geometrical modifications on the fins and in the tube shape, which can promote the separation flow and the formation of wake regions.

The turbulence model used here is the k-omega Shear-Stress Transport [12], which is a modified model based on k-omega turbulence model, proposed by Wilcox [13]. The k-omega SST is an accurate and robust model for flow with high adverse pressure gradients and swirl-flow. A very widespread model used among researchers in the field as [14], [15], [9], [16] and [17]. A robust algorithm called Coupled Algorithm was used to perform the pressure–velocity coupling, according to [11].

The thermal-hydraulic parameters to calculate the heat transfer and pressure drop depending on the geometry and on the flow conditions. The flow condition can be characterized by Reynolds number, Colburn (j) and Friction (f) factors, which are represented below [16].

$$Re = \frac{\rho U_{in} H}{\mu}. \tag{4}$$

$$f = \frac{\Delta P}{\frac{1}{2}\rho U_{in}^2} \frac{H}{L}. \tag{5}$$

$$j = \frac{h}{\rho u_{máx} c_p} Pr^{2/3}. \tag{6}$$

The equations 4-6 are adequate to compare circular and elliptical tubes since the minimum passage area is a function of elliptical tube eccentricity. Thus, the thermal-hydraulic parameters are calculated under the same reference based on fin high (H) and computational domain length (L).

The total heat transfer, pressure loss and log-mean temperature differences are defined by the equations below, according to [14].

$$Q = \dot{m} c_p \Delta \mathrm{T} = \dot{m} c_p (\bar{T}_{in} - \bar{T}_{out}). \tag{7}$$

$$\Delta p = \bar{p}_{in} - \bar{p}_{out}. \tag{8}$$

where:

$$\bar{p} = \frac{\iint_A \; p dA}{\iint_A \; dA}. \tag{9}$$

$$\bar{T} = \frac{\iint_A \; uT dA}{\iint_A \; u dA}. \tag{10}$$

The convective heat transfer coefficient is calculated by equation (11).

$$h = \frac{Q}{A_t \, \Delta T_{ln}}. \tag{11}$$

$$\Delta T_{ln} = \frac{(T_W - \bar{T}_{in}) - (T_W - \bar{T}_{out})}{ln[\frac{(T_W - \bar{T}_{in})}{(T_W - \bar{T}_{out})}]}. \tag{12}$$

2.1 Computational domain and boundary conditions

To define the computational domains and boundary conditions in this study, it is defined that x is the streamwise direction, y is the spanwise direction and z stands for the fin pitch direction, as indicated by Salviano et al. [15]. Considering computational time and cost associated with numerical simulation, the present modeling considers a compact heat exchanger under symmetry condition, with two tubes rows and a staggered-tube arrangement. Fig. 2 shows the computational domain divided into three parts: the upstream-extended region, the fin region and the downstream-extended region. The upstream region was extended one time of the main domain to ensure the inlet velocity uniformity. The downstream region was extended seven times of the main domain to avoid reversed flow. No-slip condition was assumed on fins and tubes for a constant temperature. In the downstream and upstream regions, symmetry boundary conditions were applied. An outflow (Newmann condition) boundary condition is defined at the outlet.

The present geometry is based on heat exchanger by Damavandi et al. [9], with slight modification on the inclination of the upstream and downstream extended-regions in order to obtain more stability in the numerical convergence.

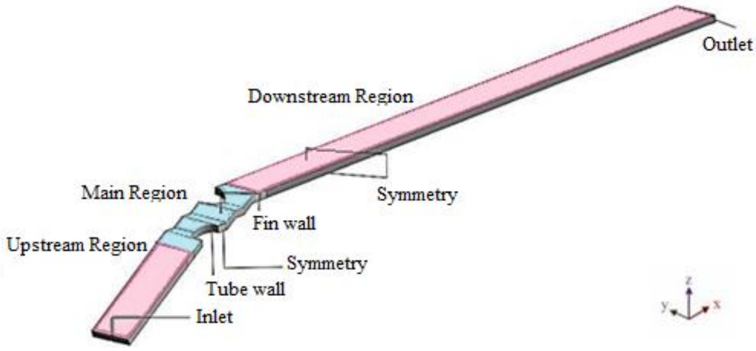

Figure 2. Computational domain of the compact heat exchanger model.

Circular and elliptical tubes were modeled in such a way that their perimeters are equal, ensuring a same heat transfer area. Frontal velocity was considered 0.5 to 2.5 m/s, which corresponds to a typical application in refrigeration systems. Vortices generators are welded on inferior wavy-fin according to Eq. (13) and (14) proposed by Lotfi et al. [17]. We can see in Fig. 3 to their positions.

$$\Delta X = \pm R_a \cos\frac{\pi}{3}. \tag{13}$$

$$\Delta Z = \pm 2R_b \sin\frac{\pi}{3}. \tag{14}$$

where: ΔX is the distance from the center of the tube in the x-axis up to the center of the VG, ΔZ is the distance from the center of the tube in the z-axis up to the center of the VG, R_a is the semi-major diameter, R_b is the semi-minor diameter.

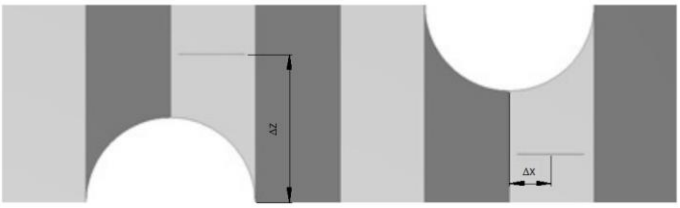

a) Circular tube

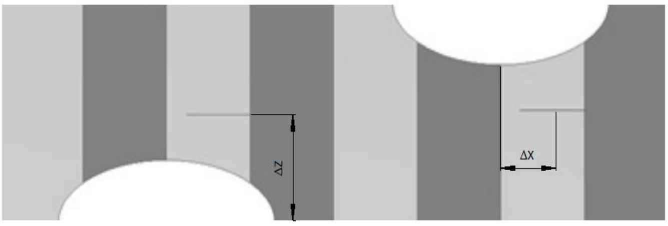

b) Elliptical tube

Figure 3. Top view of heat exchanger with vortex generators with 0° attack angle

3 Validation and grid independence

The grid independence procedure was conducted according to Celik et al. [18], by the Grid Convergence Index Methodology (GCI). Three different mesh refinements were evaluated and the results are shown in Tab.1.

Table 1. GCI calculation reports.

Cells number (Main Domain)		Refinement index, *r*	GCI_32 (%)			
			Re = 800		Re = 4000	
			J	f	J	f
Grid 1 (h1)	439.306	-				
Grid 2 (h2)	1.113.200	1,3	0.01	0.47	1.75	0.75
Grid 3 (h3)	2.451.768	1,3				

The Reynolds number for validation and GCI study is based on tube diameter. Table 1 shows the total number of cells for each grid, refinement factor *r* and GCI values. According to GCI_32 values for Friction and Colburn Factors, the higher discretization uncertainty is 1.75% for the Colburn factor and Re = 4000, which is considered small for the present work. Thus, mesh density analysis is reached and intermediate mesh can be used for the further analysis. Moreover, the average values for the y-plus [11] are shown in Tab. 2, which indicates adequate values as recommended for the turbulent model (should be close to unit).

Table 2. Grid y-plus values.

Meshes	y^+	
	Re = 800	Re = 4000
Refined (h3)	0.12	0.42
Intermediate (h2)	0.13	0.44
Coarse (h1)	0.14	0.46

The validation of the numerical modeling was performed by comparing the numerical results with the values obtained from correlations proposed by Wang et al. [19]. These correlations have a standard deviation of 10%; while the friction factor with a deviation of 15%. Fig. 4 shows that for friction factor and Re = 800 and Re = 4000, the differences are 13.7% and 2.14%, respectively, while for Colburn factor the differences are 8.03% and 0.9%, respectively. Thus, numerical modeling adopted herein could be considered robust and reliable.

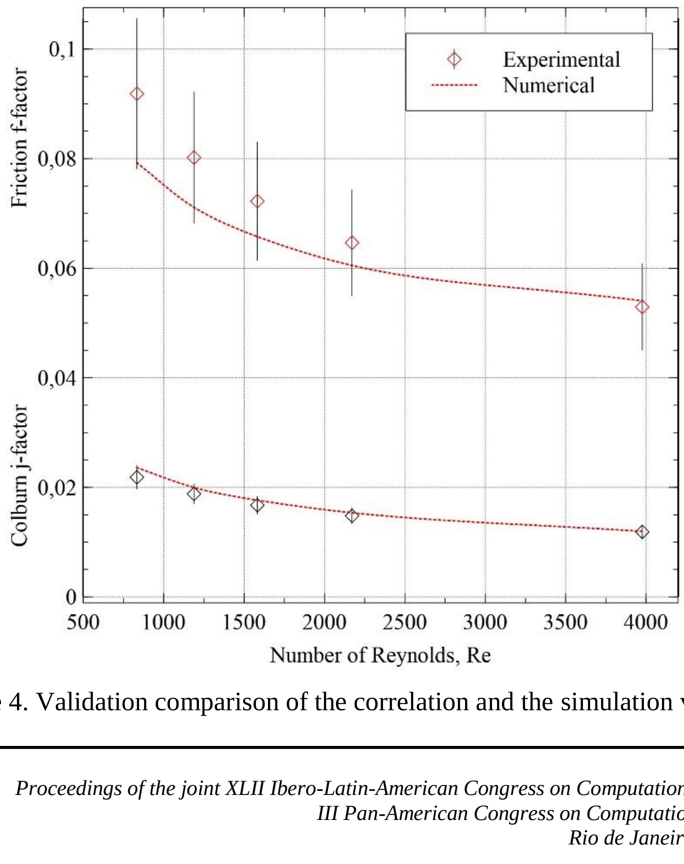

Figure 4. Validation comparison of the correlation and the simulation values.

4 Results and discussions

The profile of Colburn factor (j) and Friction factor (f) along the main domain is plotted for the Reynolds number of 150 and 600. Fig.5 shows the Colburn factor profile (j) for the configuration CD (circular tube with delta-winglet vortex generator), considering three angles of attack. Since REF is the reference case without a vortex generator.

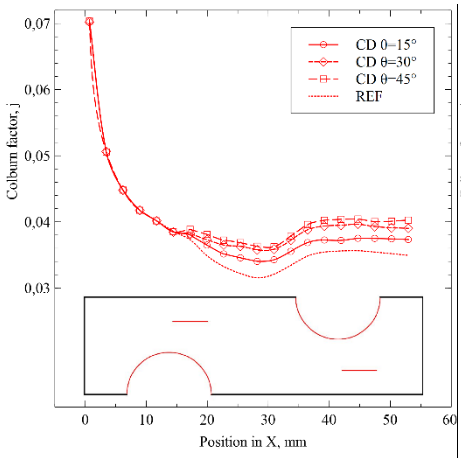

(a) Re = 150 (b) Re = 600

Figure 5. Colburn factor profile (j) in the entire main domain for the case of CD.

Figure 5 shows that for both values of the Reynolds number the heat transfer is enhanced for all angles of attack especially for 45°. The presence of the longitudinal vortex generator contributes to disrupting the boundary layer growth and to improve the mixture between cold and hot fluid streams. Fig. 6 shows the associated pressure drop profile for the CD configuration.

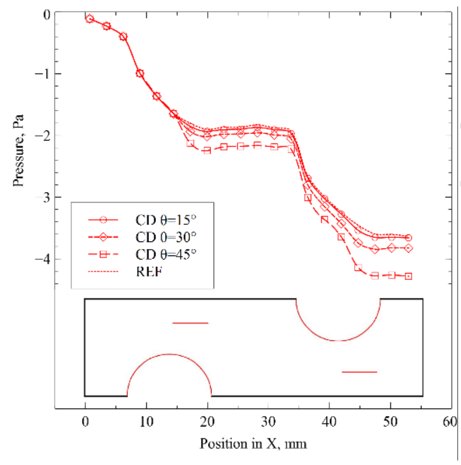

(a) Re = 150 (b) Re = 600

Figure 6. Pressure drop profile over the entire main domain for the CD case.

Fig. 6 shows that vortex generators with the angle of attack of 45° indicated more pressure drop for both Reynolds numbers. Moreover, for Reynolds number of 600, a small difference is verified for the angle of attack of 15º and 30º, which is not verified for Reynolds number of 150.

The same behavior is verified for the configuration with circular tube and rectangular-winglet vortex generator (CR), as shown in Fig. 7 and Fig. 8.

Fig. 7 shows significant increase in heat transfer, independent of the angle of attack and the Reynolds number. The impact of the rectangular-winglet vortex generator is more evident at position x = 15 mm for the angle of attack of 45º at Reynolds number of 600. The rectangular-winglet vortex generator promotes a greater heat transfer intensification and, consequently, this leads to a greater pressure drop as can be seen in Fig. 8, for both Reynolds number. The case with a 45° angle of attack showed a large pressure drop in relation to the reference case. For low Reynolds number, the pressure drop is also significant, although heat transfer was less pronounced than for high Reynolds number. This corroborate the difficulty of intensifying heat transfer at low Reynolds number with moderate pressure loss.

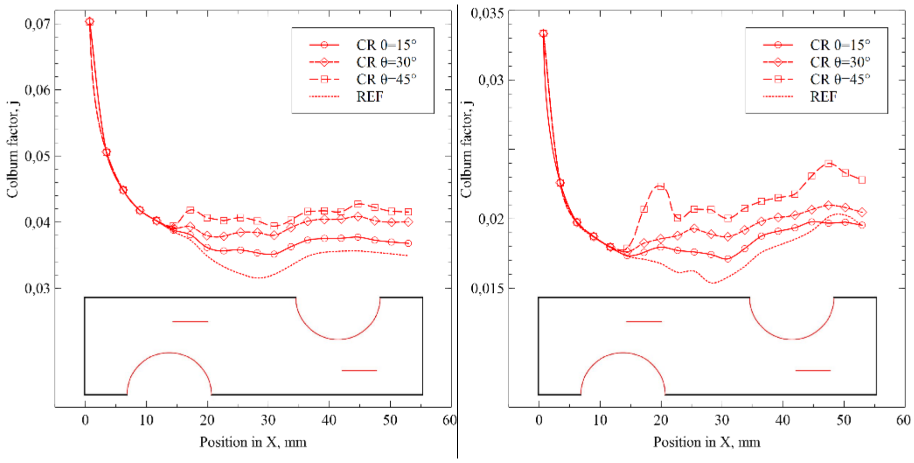

(a) Re = 150 (b) Re = 600

Figure 7. Colburn factor profile (j) along the main domain for the CR case.

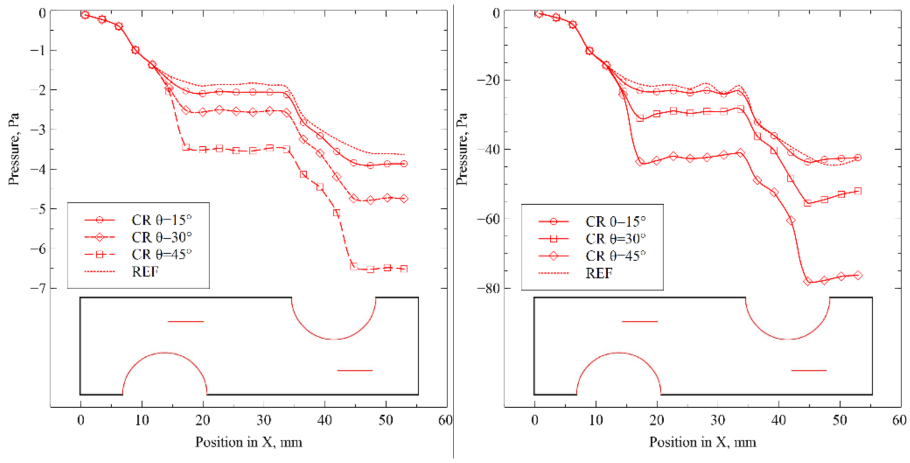

(a) Re = 150 (b) Re = 600

Figure 8. Pressure drop profile along the main domain for the CR case.

Fig. 9 shows the Colburn factor (j) for configuration with elliptical tube with delta-winglet vortex generator (ED), and Fig. 8 shows its pressure drop profile. As can be seen, the Colburn factor for the angles of attack of 30° and 45° are similar, with slight increases in heat transfer compared to the reference configuration. The impact of the angle of attack is slight on Colburn factor for elliptical tubes for both Reynolds number. Moreover, the enhancement heat transfer for the elliptical tube is lower than that reached for circular tube. Fig. 10 shows that the pressure drop for the configuration with angle of attack of 15º is numerically insignificant when compared to the reference configuration, showing that the flow dynamics imposed by the wavy-fin is more significant than the effects produced by the vortex generators for small angles of attack. The highest pressure drop is observed for the angle of attack of 45°.

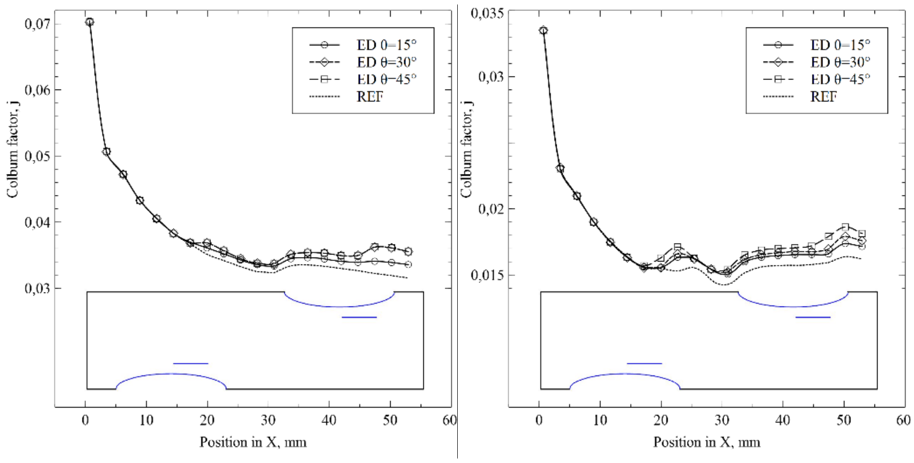

(a) Re = 150 (b) Re = 600

Figure 9. Colburn factor profile (j) along the main domain for the ED case.

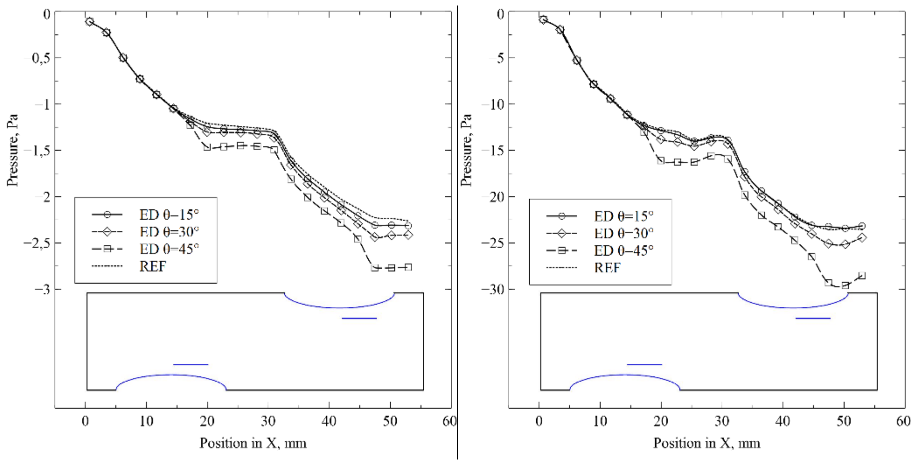

(a) Re = 150 (b) Re = 600

Figure 10. Pressure drop profile along the main domain for the ED case.

Similarly, the Fig. 11 shows the Colburn factor (j) along the main domain for the configuration with elliptical tube with rectangular-winglet vortex generator (ER) for different angles of attack of the vortex generator for Reynolds number of 150 and 600. For all configurations investigated, the enhancement heat transfer for ER is higher than the reference configuration and also higher than ED configurations. Moreover, the angle of attack influenced the heat transfer more than for ED configuration even at a smaller angle of attack. However, the higher pressure drop is also verified for ER configurations, Fig. 12. Evidently, the higher pressure drop is observed for the angle of attack of 45º. Although the pressure drop of the ER with angle of attack of 15º is similar to reference configuration for Reynolds number of 600, Fig. 12, the heat transfer is increased as shown in Fig. 11.

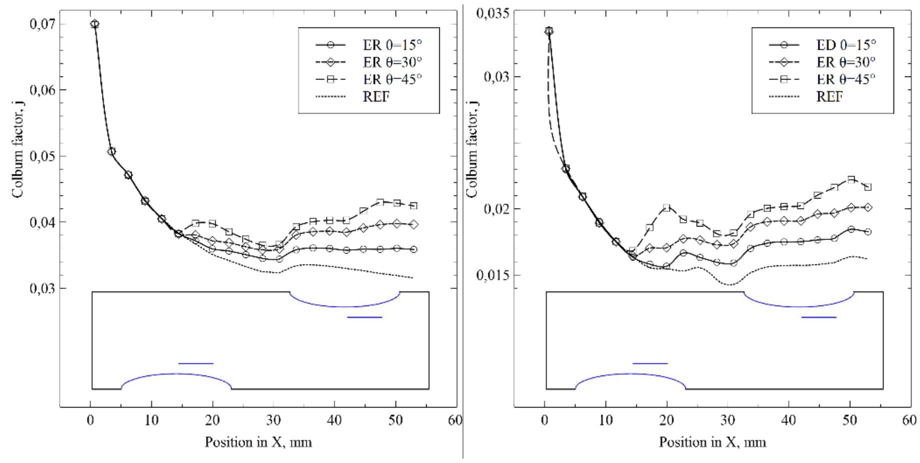

(a) Re = 150 (b) Re = 600

Figure 11. Colburn profile along the entire main domain for the ER case.

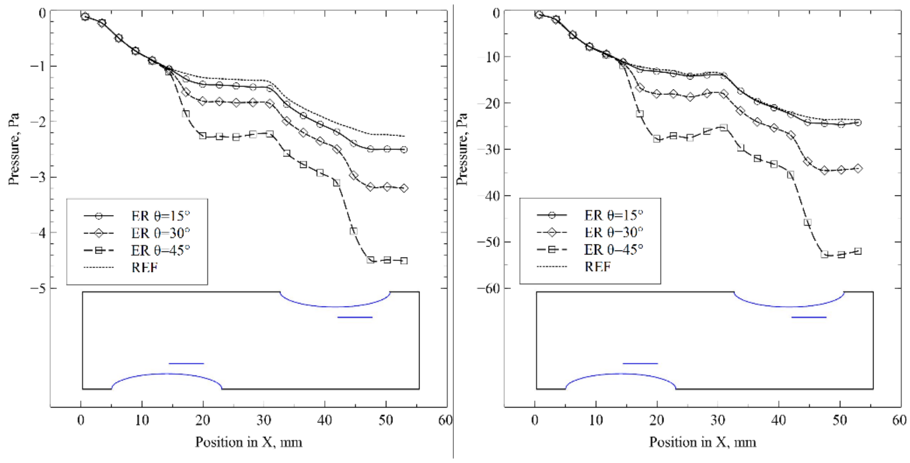

(a) Re = 150 (b) Re = 600

Figure 12. Pressure drop profile along the main domain for the ER case.

5 Conclusions

In this work, a study of a numerical simulation of a wavy-fin compact heat exchanger combined with longitudinal vortex generators was performed to enhance the heat transfer. Circular and elliptical tubes were investigated for Reynolds numbers of 150 and 600 (based on fin-pitch) for staggered arrangement. Based on Colburn factor and Friction factor, the mains conclusions are presented:

- The enhancement heat transfer is reached for higher angle of attack, although higher pressure drop is also observed;
- Vortex generator is an effective device to enhance the heat transfer especially for the rectangular and higher angle of attack;
- Rectangular-winglet vortex generator enhances the heat transfer more than delta-winglet vortex generator for both circular and elliptical tubes;
- Enhance the heat transfer at lower Reynolds number is harder than at higher Reynolds number.

References

[1] E. Pis'mennyi, G. Polupan, I. Carvajal-Mariscal, F. Sanchez-Silva, and I. Pioro, *Handbook for Transversely Finned Tube Heat Exchanger Design*. 2016.

[2] F. P. Incropera and D. P. Witt, *Fundamentos de transferência de calor e massa*, 6ª edição. Rio de Janeiro: LTC - Livros Técnicos e Científicos Editora S.A, 2008.

[3] T. Alam and M. H. Kim, "A comprehensive review on single phase heat transfer enhancement techniques in heat exchanger applications," *Renew. Sustain. Energy Rev.*, vol. 81, no. August 2017, pp. 813–839, 2018, doi: 10.1016/j.rser.2017.08.060.

[4] A. A. Bhuiyan and A. K. M. S. Islam, "Thermal and hydraulic performance of finned-tube heat exchangers under different flow ranges: A review on modeling and experiment," *Int. J. Heat Mass Transf.*, vol. 101, pp. 38–59, 2016, doi: 10.1016/j.ijheatmasstransfer.2016.05.022.

[5] C. C. Wang, Y. J. Chang, and C. J. Lee, "Investigation of wavy fin-and-tube heat exchangers: A contribution to databank," *Exp. Heat Transf.*, vol. 12, no. 1, pp. 73–89, 1999, doi: 10.1080/089161599269825.

[6] L. Tian, Y. He, P. Chu, and W. Tao, "Numerical study of flow and heat transfer enhancement by using delta winglets in a triangular wavy fin-and-tube heat exchanger," *J. Heat Transfer*, vol. 131, no. 9, pp. 1–8, 2009, doi: 10.1115/1.3139106.

[7] M. Fiebig, "Vortices, generators and heat transfer," *Chem. Eng. Res. Des.*, vol. 76, no. 2, pp. 108–123, 1998, doi: 10.1205/026387698524686.

[8] C. C. Wang, J. Lo, Y. T. Lin, and M. S. Liu, "Flow visualization of wave-type vortex generators having inline fin-tube arrangement," *Int. J. Heat Mass Transf.*, vol. 45, no. 9, pp. 1933–1944, 2002, doi: 10.1016/S0017-9310(01)00289-7.

[9] M. Darvish Damavandi, M. Forouzanmehr, and H. Safikhani, "Modeling and Pareto based multi-objective optimization of wavy fin-and-elliptical tube heat exchangers using CFD and NSGA-II algorithm," *Appl. Therm. Eng.*, vol. 111, pp. 325–339, 2017, doi: 10.1016/j.applthermaleng.2016.09.120.

[10] M. M. Aslam Bhutta, N. Hayat, M. H. Bashir, A. R. Khan, K. N. Ahmad, and S. Khan, "CFD applications in various heat exchangers design: A review," *Appl. Therm. Eng.*, vol. 32, no. 1, pp. 1–12, 2012, doi: 10.1016/j.applthermaleng.2011.09.001.

[11] ANSYS FLUENT, "ANSYS Fluent," *ANSYS Inc., USA*, p. 0, 2013.

[12] F. Menter, "Zonal Two Equation k-w Turbulence Models For Aerodynamic Flows," Jul. 1993, doi: 10.2514/6.1993-2906.

[13] D. C. Wilcox, "Reassessment of the scale-determining equation for advanced turbulence models," *AIAA J.*, 1988, doi: 10.2514/3.10041.

[14] L. O. Salviano, D. J. Dezan, and J. I. Yanagihara, "Thermal-hydraulic performance optimization of inline and staggered fin-tube compact heat exchangers applying longitudinal vortex generators," *Appl. Therm. Eng.*, vol. 95, no. November, pp. 311–329, 2016, doi: 10.1016/j.applthermaleng.2015.11.069.

[15] L. O. Salviano, D. J. Dezan, and J. I. Yanagihara, "Optimization of winglet-type vortex generator positions and angles in plate-fin compact heat exchanger: Response Surface Methodology and Direct Optimization," *Int. J. Heat Mass Transf.*, vol. 82, no. March 2018, pp. 373–387, 2015, doi: 10.1016/j.ijheatmasstransfer.2014.10.072.

[16] R. Deepakkumar and S. Jayavel, "Air side performance of finned-tube heat exchanger with combination of circular and elliptical tubes," *Appl. Therm. Eng.*, vol. 119, pp. 360–372, 2017, doi: 10.1016/j.applthermaleng.2017.03.082.

[17] B. Lotfi, M. Zeng, B. Sundén, and Q. Wang, "3D numerical investigation of flow and heat transfer characteristics in smooth wavy fin-and-elliptical tube heat exchangers using new type vortex generators," *Energy*, vol. 73, pp. 233–257, 2014, doi: 10.1016/j.energy.2014.06.016.

[18] I. B. Celik, U. Ghia, P. J. Roache, C. J. Freitas, H. Coleman, and P. E. Raad, "Procedure for estimation and reporting of uncertainty due to discretization in CFD applications," *J. Fluids Eng. Trans. ASME*, vol. 130, no. 7, pp. 0780011–0780014, 2008, doi: 10.1115/1.2960953.

[19] C. C. Wang, W. L. Fu, and C. T. Chang, "Heat transfer and friction characteristics of typical wavy fin-and-tube heat exchangers," *Exp. Therm. Fluid Sci.*, vol. 14, no. 2, pp. 174–186, Feb. 1997, doi: 10.1016/S0894-1777(96)00056-8.